ELSEVIER Journal of Electron Spectroscopy and Related Phenomena 101–103 (1999) 119–124

JOURNAL OF ELECTRON SPECTROSCOPY and Related Phenomena

Photofragmentation of OCS at the S 1s edge

John J. Neville*, Tolek Tyliszczak, Adam P. Hitchcock

Department of Chemistry, McMaster University, Hamilton, ON, Canada L8S 4M1

Abstract

The photofragmentation of carbonyl sulphide following sulphur 1s excitation has been investigated using monochromated synchrotron radiation and ion time-of-flight mass spectroscopy. Photoion branching ratios indicate that fragmentation to atomic ions increases at the onset of S 1s excitation and that the yield of multiply charged ions increases at the onset of S 1s excitation and again at the S 1s ionization threshold. Cleavage of the carbon–sulphur bond is favoured over cleavage of the oxygen–carbon bond both above and below the sulphur 1s ionization threshold. The multi-coincident detection of up to three photoions per ionization event is used to identify the fragmentation channels following S 1s→π* excitation and explore the fragmentation dynamics.

Keywords: Photoionization; Photofragmentation dynamics; Core excitation; OCS

1. Introduction

The excitation or ionization of a core electron produces a highly excited electronic state that relaxes typically by Auger processes to yield a multiply ionized molecule. Fragmentation of this molecular ion follows as a consequence of the loss of bonding electrons and the presence of multiple positive charges. If the core hole is a deep one such as S 1s, the electronic relaxation most often involves an Auger cascade, resulting in states of high total charge and leading to extensive molecular fragmentation. In the case of carbonyl sulphide (OCS), Esser et al. [1] have observed that for photoexcitation above the S 1s ionization threshold complete fragmentation into three positively charged atomic constituents dominates, with the total charge as great as +7. Multi-coincidence ion time-of-flight (TOF) mass spectrometry provides an effective method for studying the fragmentation process [2,3]. For example, the detection of up to three photoions from a single OCS photofragmentation event identifies completely the fragmentation channel.

In a recent pair of publications Esser et al. [1] and Ankerhold et al. [4] have reported photoelectron–multiphotoion coincidence measurements of OCS and CS_2 photoexcited near the S 1s edge, focusing on the total ionic charge spectra and the electronic relaxation of the core hole in the first case and on the dissociation channels in the second case. In the second study, branching ratios of specific fragmentation channels, including an estimate of channels containing a neutral fragment, were reported and the fragmentation kinematics following photoexcitation above the S 1s ionization threshold were studied in detail. Ankerhold et al. [4] found that multiphotoion coincidence data were reproduced well using a Coulomb explosion model to simulate the fragmentation dynamics. In the present study, we investigate

*Corresponding author.
E-mail address: neville@mcmaster.ca (J.J. Neville)

0368-2048/99/$ – see front matter
PII: S0368-2048(98)00422-8

the photoion branching ratios following S 1s excitation of OCS, focusing on the discrete excitation region, and examine the fragmentation dynamics below the S 1s ionization threshold at the S 1s→π* excitation at 2472 eV photon energy.

2. Experimental method

The measurements were performed using the double-crystal monochromator beamline (beamline 091) of the Canadian Synchrotron Radiation Facility (CSRF) located at the Synchrotron Radiation Center (SRC), University of Wisconsin at Madison. A pair of InSb crystals provided tunable monochromated synchrotron radiation in the range 1740–4200 eV with an energy resolution of ~1 eV FWHM in the vicinity of the S 1s edge.

Mass-resolved photoion yields were obtained using a Wiley–McLaren type [5] TOF mass spectrometer mounted perpendicular to the polarization vector of the incident synchrotron radiation. Ions were extracted electrostatically into a field-free drift tube 20 cm in length which is terminated by a pair of 25-mm-diameter microchannel plates used for ion detection. The branching ratio measurements were performed using a 680 V/cm extraction field pulsed at 100 kHz with a 50% duty cycle. A marker signal synchronized with the onset of the extraction pulse was used as the TOF start signal. In contrast, the multi-photoion coincidence measurements at the S 1s→π* transition were performed using a continuous 640 V/cm extraction field and a detected photoelectron as the TOF start signal. The photoelectron–photoion coincidence (PEPICO) mode provides greater efficiency for the detection of ion triplets while the pulsed extraction mode has been found to provide more quantitative photoion branching ratios [6]. The photoion flight times were determined using a TOLMAR time-to-digital convertor (TDC) with a time resolution of 12.5 ns and a 180 ns dead time. The gaseous sample was introduced into the experimental chamber through a high-aspect-ratio stainless steel needle oriented perpendicular to both the TOF axis and the X-ray beam. The sample pressure was maintained at $\sim 4\times10^{-6}$ Torr during data acquisition. The base pressure was less than 1×10^{-7} Torr.

3. Photoion branching ratios

The total ion yield spectrum (TIY) of OCS near the S 1s ionization threshold, obtained in the pulsed extraction mode, is compared in Fig. 1 with the photoion branching ratios derived from TOF spectra collected at each photon energy. It is not possible to separate the branching ratios of O^+ and S^{2+} or O^{2+} and S^{4+} because these ion pairs have identical mass/charge ratios and therefore appear at the same flight times in the TOF spectra. The S 1s binding energy of 2478.7 eV indicated in Fig. 1 was estimated by Perera and LaVilla [7] from the sulphur K_β emission spectrum of OCS and valence-shell UPS data [8]. The energies and assignments of the TIY spectral features are listed in Table 1 and follow the assignments of Perera and LaVilla [7].

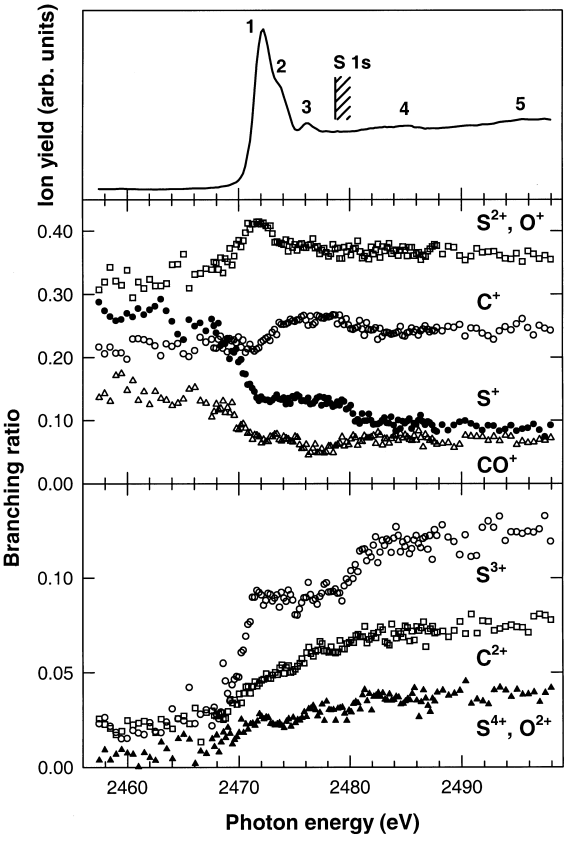

Fig. 1. Total ion yield and photoion branching ratios of OCS near the S 1s ionization threshold. The S 1s binding energy estimated by Perera and LaVilla [7] is indicated.

Table 1
Energies and assignments of S 1s excitation features of OCS. The term values have been calculated using the S 1s binding energy of 2478.7 eV estimated by Perera and LaVilla [7]

Feature	Photon energy (eV)	Term value (eV)	Assignment
1	2472.1	6.6	3π
2	2473.8	4.9	$5\sigma+6\sigma$
3	2476.2	2.5	4p Rydberg
4	2485	−6	
5	2496	−17	

The branching ratios of all ions observed with significant populations in the TOF spectra are shown in Fig. 1. In addition, weak peaks corresponding to CS^+ and OCS^+ are observed, as seen in the PEPICO TOF spectra of OCS excited with 2472 eV photons (S 1s→3π excitation) shown in Fig. 2. This contrasts with the recent study by Ankerhold et al. [4] in which neither of these ions were detected. There is also a very weak peak in the TOF spectrum at a flight time of ~0.7 μs, corresponding to a mass/charge ratio of 4. C^{3+} seems the most reasonable assignment for this peak because of the high charges required on oxygen or sulphur to produce ions having the appropriate mass/charge ratio.

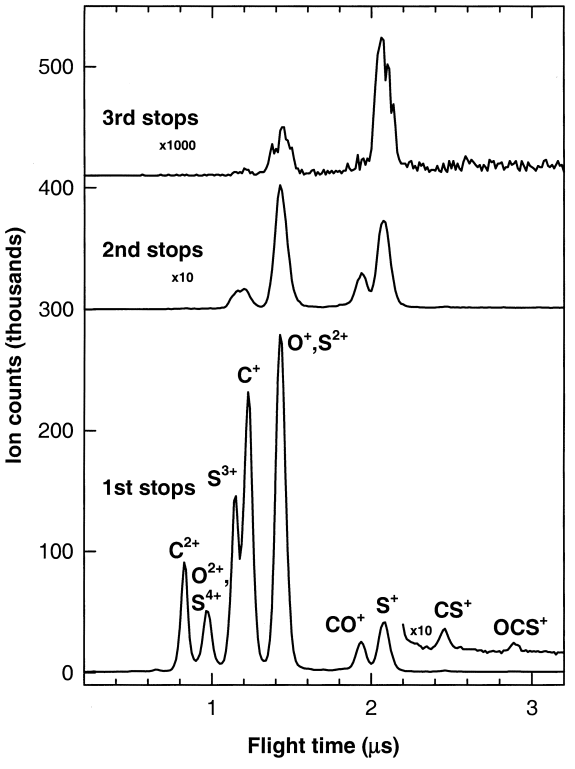

Fig. 2. Photoelectron–multiphotoion coincidence time-of-flight spectra of OCS following excitation at 2472 eV, the S 1s→π* transition energy.

The branching ratio spectra can generally be divided into three regions: that below the onset of S 1s excitation at ~2470 eV, the S 1s discrete excitation region and the S 1s ionization continuum. The photoion branching ratios are approximately constant below the onset of S 1s excitation. The relative yield of multiply charged ions increases at the onset of S 1s excitation, with the branching ratios becoming approximately constant again above the S 1s ionization potential. The degree of fragmentation also increases with S 1s excitation as indicated by the steady decrease in the CO^+ branching ratio between the S 1s→π* resonance and the ionization limit.

Both the C^{2+} and S^{4+}/O^{2+} branching ratios increase steadily from the onset of S 1s excitation to the S 1s ionization threshold, with no obvious structure corresponding to the various core-excited electronic states accessed in this photon energy range. Similar behaviour was observed by Esser et al. [1] in the total ion charge spectra of OCS in the vicinity of S 1s excitation and was attributed to an increased probability of shake-off of the excited photoelectron as its binding energy decreases.

In contrast to the steady decrease of the CO^+ branching ratio and steady increase of the C^{2+} and S^{4+}/O^{2+} branching ratios through the discrete excitation region, the branching ratios of the other ions are more structured. The creation of the S 1s core hole increases the number of potential decay steps in the Auger cascade and results in a greater average total charge following relaxation of the core hole. Esser et al. [1] found that the average total ionic charge increases from +3.2 just below the S 1s edge to +4.4 above the S 1s ionization threshold. Reflecting this, the S^+ branching ratio displays a step-like behaviour, decreasing sharply at the S 1s→3π resonance and decreasing again at the ionization limit. The S^{3+} branching ratio exhibits complementary behaviour, increasing with the onset of both S 1s excitation and ionization. The branching ratios for both ions, however, are essentially constant throughout the S 1s excitation region and do not indicate any state-specific variation in the fragmentation of OCS.

The second 'step' in the S^+ and S^{3+} branching ratios begins at the S 1s ionization limit but the branching ratios do not become constant until 3 or 4 eV above the ionization limit. This was also observed by Esser et al. [1] in the total charge spectra of OCS measured near the S 1s edge and was attributed to post-collision interaction.

The combined S^{2+}/O^+ and the C^+ branching ratios both increase in the S 1s discrete excitation region and then decrease at higher photon energy. Unlike the branching ratios of the other ions, that of C^+ does not change at the 3π resonance but instead only begins to increase at the 5σ resonance. Considering that the CO^+ branching ratio does begin to decrease at the 3π resonance, this suggests that production of CO^+ decreases in favour of neutral carbon and O^+ with S $1s\rightarrow3\pi$ excitation, but that C^+ and O^+ or C^+ and neutral oxygen are favoured following S $1s\rightarrow5\sigma$ and S $1s\rightarrow6\sigma$ excitation. The slight drop in the relative C^+ yield at the S 1s ionization limit reflects the increased production of C^{2+}.

The combined S^{2+}/O^+ branching ratio also exhibits a clear state dependency, with the relative abundance of these ions greatest following S $1s\rightarrow3\pi$ excitation. This is consistent with the proposal presented above that the increased cleavage of the carbon–oxygen bond that follows S $1s\rightarrow3\pi$ excitation leads preferentially to production of neutral carbon and O^+. Note that Ankerhold et al. [4] attributed the state-dependent variations they observed in ion fragmentation channel branching ratios solely to variations in the relative contributions of S 1s excitation and ionization of lower binding energy shells. However, the magnitude of the variation of the S^{2+}/O^+ branching ratio observed in the present data in the S 1s discrete excitation region is too great to be accounted for in this manner.

The photoion branching ratios exhibiting the most dramatic variations are those of S^+ and S^{3+}. The fact that sulphur is the core-excited atom suggests a 'memory effect', in which the core-excited centre carries the bulk of the charge. However, it is important to note that the valence electrons of sulphur will be less strongly bound than those of carbon and oxygen, so it is reasonable for the sulphur fragment ions to be more highly charged even in the absence of any core-hole memory effect. Similarly, the yield of CO^+ greatly exceeds that of CS^+, which is almost negligible. One interpretation is that cleavage of the bond to the core-excited atom is the more probable fragmentation process. However, the CS^+ ion yield is minimal even before the onset of S 1s excitation, suggesting that the relative abundance of CO^+ and CS^+ is a function of the relative strengths of the C=O and C=S bonds rather than the site of core excitation.

4. Fragmentation following S $1s\rightarrow3\pi$ excitation

TOF spectra of OCS photoexcited with 2472 eV photons, collected in photoelectron–multiphotoion mode, are shown in Fig. 2. Separate TOF spectra are shown for all first, second and third ions detected. The relative intensities of these three spectra illustrate the challenge of collecting good quality data sets of photoelectron–triple photoion coincidences. The ion detection efficiency of the apparatus used in the present work is estimated to be $\approx 10\%$, accounting for the relative intensity of the first and second stop signals. However, the number of third stops detected is even lower than expected based upon the ion detection efficiency alone. This is most likely because of photoionization events in which one of the ions has a kinetic energy perpendicular to the TOF axis sufficiently large to escape without detection.

By plotting two-dimensional maps of the correlations between the flight times of two ions from the same ionization event, insight into the fragmentation dynamics may be obtained [2–4]. This is a consequence of the fact that the flight time of each ion, a function primarily of its mass/charge ratio, is modified by the initial kinetic energy of the ion along the TOF axis. Ion TOF correlation maps for OCS following S $1s\rightarrow3\pi$ excitation are shown in Fig. 3. In the upper-left panel, the correlations between the second and first ions detected are plotted. The majority of the coincidences are between atomic ions but complete fragmentation channels involving one atomic and one molecular ion are also observed (i.e. S^{3+}, CO^+ and S^{2+}, CO^+, features E and F). Note that the relatively long dead time of the TDC used for these measurements (180 ns) precludes the detection of several fragmentation channels, for

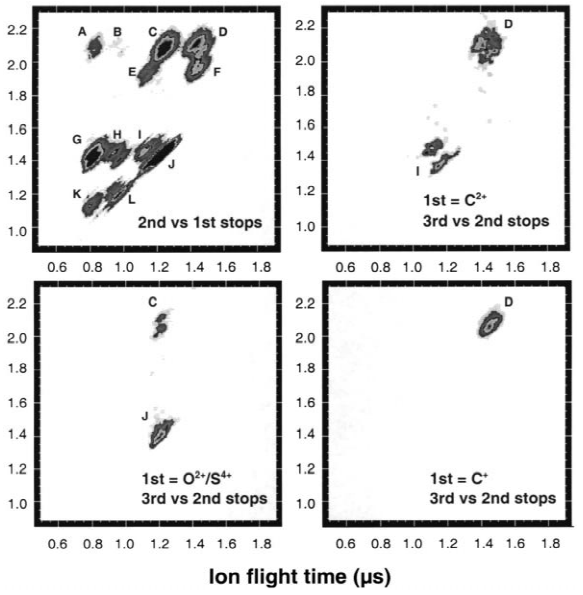

Fig. 3. Fragment ion correlations following excitation of OCS at 2472 eV, the S 1s→π* transition energy. The labelled features are: A (C^{2+}, S^{+}); B (O^{2+}, S^{+}); C (C^{+}, S^{+}); D (O^{+}, S^{+}); E (S^{3+}, CO^{+}); F (S^{2+}, CO^{+}); G (C^{2+}, S^{2+}/O^{+}); H (S^{4+}, O^{2+})/(O^{2+}, S^{+}); I (S^{3+}, O^{+}); J (C^{+}, O^{+}/S^{2+}); K (C^{2+}, S^{3+}) and L (O^{2+}, S^{3+})/(O^{2+}/S^{4+}, C^{+}).

example CO^{+}, S^{+} and channels involving O^{2+} and S^{4+}, S^{3+} and C^{+}, and O^{+} and S^{2+}.

The remaining three panels of Fig. 3 show the TOF correlations between the second and third ions detected for selected first ions. Although the second versus first stops data set consists of over 225 000 ionization events for which at least two ions were detected, the number of triple-ion events detected was only 616 with C^{2+} as the first ion detected, 477 with O^{2+} or S^{4+} and 1233 with C^{+}.

One advantage of detecting all of the ions produced in a fragmentation event is that ambiguities regarding the identity of ions having the same mass/charge ratio can in many cases be resolved. For example, the identity of the first detected ion in the data set shown in the lower-left panel of Fig. 3 cannot be determined from its flight time alone. However, in the case of feature C, which corresponds to the C^{+}, S^{+} ion pair, the first ion must be O^{2+} since the sulphur atom is already accounted for.

Obtaining detailed information concerning the fragmentation dynamics of polyatomic molecules requires simulation of fragmentation models and comparison with the experimental data, but some insight can be obtained from the shapes of the ion-pair correlation features. Fragmentation processes in which ions are produced with sufficient kinetic energy that they will not be detected if their original trajectory is perpendicular to the TOF axis will give rise to double-peaked structures, as is seen, for example, for the S^{3+}, O^{+} coincidence (feature I) when C^{2+} is the first ion detected. Comparing the orientations of the double-peaked (C^{2+}), S^{3+}, O^{+} and (O^{2+}), C^{+}, S^{+} features (I and C, respectively), it can be inferred that the C^{+} of (O^{2+}), C^{+}, S^{+} is produced with low kinetic energy, as would be expected for the central ion in a linear three-body Coulomb explosion, while S^{3+} and O^{+} are produced with significant kinetic energy in opposite directions in the C^{2+}, S^{3+}, O^{+} fragmentation channel.

5. Conclusions

Photoion branching ratio measurements of OCS reveal increases in the degree of fragmentation and the relative yield of multiply charged ions following S 1s excitation and ionization. Although most of the branching ratios do not display any state dependencies in the S 1s discrete excitation region, the C^{+} and S^{2+}/O^{+} branching ratios indicate a preference towards production of O^{+} rather than C^{+} following S 1s→3π excitation. The detection of up to three photoions in coincidence enables the complete identification of the fragmentation channel and often eliminates ambiguities in the assignment of signals from ions having the same mass/charge ratio.

Acknowledgements

Financial support for this work was provided by NSERC (Canada). We thank A.L.D. Kilcoyne for his expert work in fabricating the time-of-flight/TDC measurement system and G. Retzlaff (CSRF–SRC) for his assistance with the measurements. JJN acknowledges NSERC for receipt of a postdoctoral fellowship. This work is based upon research conducted at the Synchrotron Radiation Center, Uni-

versity of Wisconsin–Madison, which is supported by the NSF under Award No. DMR-95-31009.

References

[1] B. Esser, U. Ankerhold, N. Anders, F. von Busch, J. Phys. B: At. Mol. Phys. 30 (1997) 1191–1206.
[2] I. Nenner, P. Morin, in: U. Becker, D.A. Shirley (Eds.), VUV and Soft X-ray Photoionization, 1996, pp. 291–354.
[3] P. Morin, M. Simon, C. Miron, N. Leclercq, D.L. Hansen, J. Electron Spectrosc. Relat. Phenom. 93 (1998) 49–60.
[4] U. Ankerhold, B. Esser, F. von Busch, J. Phys. B: At. Mol. Phys. 30 (1997) 1207–1222.
[5] W.C. Wiley, I.H. McLaren, Rev. Sci. Instrum. 26 (1955) 1150–1157.
[6] J.J. Neville, A.P. Hitchcock, A. Jürgensen, R.G. Cavell, in preparation.
[7] R.C.C. Perera, R.E. LaVilla, J. Chem. Phys. 81 (1984) 3375–3382.
[8] A.W. Potts, G.H. Fattahallah, J. Phys. B: At. Mol. Phys. 13 (1980) 2545.